

Mixed-metal cluster chemistry III¹. P–C activation at tungsten–triiridium cores; X-ray crystal structures of $[\text{CpWIr}_3\{\mu_3\text{-}\eta^2\text{-PPh}(\text{C}_6\text{H}_4)\}\{\mu\text{-CO}\}_2(\text{CO})_7]$ and $[\text{CpWIr}_3\{\mu_3\text{-}\eta^2\text{-PPh}(\text{C}_6\text{H}_4)\}\{\mu\text{-CO}\}_2(\text{CO})_6(\text{PPh}_3)]$

Susan M. Waterman^a, Vicki-Anne Tolhurst^b, Mark G. Humphrey^{a,*}, Brian W. Skelton^c, Allan H. White^c

^a Department of Chemistry, Australian National University, Canberra, A.C.T. 0200, Australia

^b Department of Chemistry, University of New England, Armidale, N.S.W. 2351, Australia

^c Department of Chemistry, University of Western Australia, Nedlands, W.A. 6907, Australia

Received 27 September 1995

Abstract

The thermolysis of $[\text{CpWIr}_3(\mu\text{-CO})_3(\text{CO})_7(\text{PPh}_3)]$ in refluxing toluene gives $[\text{CpWIr}_3\{\mu_3\text{-}\eta^2\text{-PPh}(\text{C}_6\text{H}_4)\}\{\mu\text{-CO}\}_2(\text{CO})_7]$ (**1**) in good yield (56%), together with $[\text{CpWIr}_3(\text{CO})_{11}]$ (**2**) (32%); an analogous reaction with $[\text{CpWIr}_3(\mu\text{-CO})_3(\text{CO})_6(\text{PPh}_3)_2]$ gives **1** (23%) and $[\text{CpWIr}_3\{\mu_3\text{-}\eta^2\text{-PPh}(\text{C}_6\text{H}_4)\}\{\mu\text{-CO}\}_2(\text{CO})_6(\text{PPh}_3)]$ (**3**) (39%). Products **1** and **3** (in 15 and 44% yield respectively) are also obtained from heating $[\text{CpWIr}_3(\mu\text{-CO})_3(\text{CO})_5(\text{PPh}_3)_3]$. Both **1** and **3** have been structurally characterized. The structural studies show that orthometallation has occurred, to afford products with (phenylphosphido)phenyl-*P,C* ligands capping the triiridium faces. In **3**, the intact PPh_3 resides at an iridium ligated by the phosphorus of the capping group. Attempts to effect further P–C cleavage of **1** (pyrolysis, photolysis, reaction with trimethylamine-*N*-oxide) were unsuccessful, as were attempts to effect C–H activation at the analogous $[\text{CpWIr}_3(\mu\text{-CO})_3(\text{CO})_7(\text{PMe}_3)]$.

Keywords: Tungsten; Iridium; Cluster; Crystal structure; Orthometallation

1. Introduction

Transition-metal mediated phosphorus–carbon bond cleavage is of intrinsic interest, as well as relevant to homogeneous catalyst deactivation [2]. The fragments resulting from such P–C cleavage are frequently stabilized on multimetallic frameworks, and so clusters with phosphine ligands have been an abundant source of such species. Not surprisingly then thermolyses of ruthenium [3–6] or osmium [3b,4] clusters proceed by P–C bond-breaking, although the chemistry of the lighter metal is complicated by competitive Ru–Ru cleavage. More recent work by Deeming and coworkers has delineated the fragmentation pathway for PRPh_2 ($\text{R} = \text{Me}, \text{Ph}$) on triosmium clusters, with reaction pro-

ceeding by way of orthometallated reaction intermediates as in Scheme 1.

Thermolysis of $[\text{Ir}_4(\text{CO})_{12}]$ with triphenylphosphine gives a cluster bearing a phenylphosphinidene ligand [5]; however, no orthometallated phosphine derived ligands have been identified thus far in the tetrairidium system, although $[\text{Ir}_4(\mu\text{-H})(\mu_3\text{-}\eta^2\text{-Ph}_2\text{PCH}_2\text{CH}_2\text{-PPhC}_6\text{H}_4)\{\mu\text{-CO}\}_3(\text{CO})_4(\eta^2\text{-dppe})]$ with an orthometallated phenyl group has been reported [6]. Despite comprehensive investigations with homometallic clusters, little is known of P–C cleavage on mixed-metal clusters. We have recently reported the facile high-yielding syntheses of the specifically substituted clusters $[\text{CpWIr}_3(\mu\text{-CO})_3(\text{CO})_{8-n}(\text{PPh}_3)_n]$ ($n = 1$ to 3) [1]. As part of our ongoing investigations contrasting reactivity at the tetrahedral tungsten–iridium clusters to that at the parent tetrairidium system, we have examined the thermolyses of these clusters, and report below the charac-

* Corresponding author.

¹ For Part II, see Ref. [1].

terization by single crystal X-ray studies of the resultant orthometallated products.

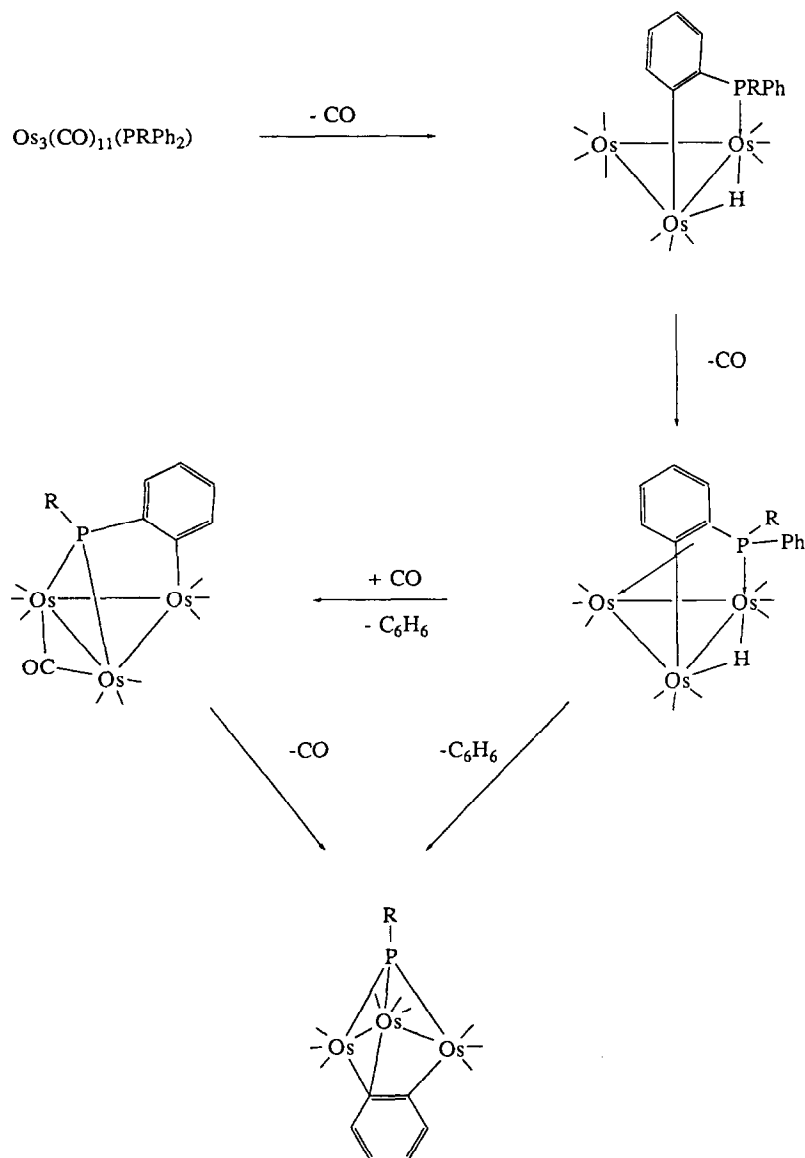
2. Results and discussion

2.1. Syntheses and characterization of 1 and 3

Heating $[\text{CpWIr}_3(\mu\text{-CO})_3(\text{CO})_7(\text{PPh}_3)]$ in toluene for 15 min gave one major and one minor product on purification by preparative thin-layer chromatography. The minor band, $[\text{CpWIr}_3(\text{CO})_{11}]$ (**2**), was isolated in 32% yield, and its identity confirmed by FTIR spectroscopy. The major product was obtained in 56% yield as dark purple crystals of $[\text{CpWIr}_3\{\mu_3\text{-}\eta^2\text{-PPh}(\text{C}_6\text{H}_4)\}(\mu\text{-CO})_2(\text{CO})_7]$ (**1**). The spectral data are sufficient to establish the molecular composition but not

the specific ligation sites. The solution FTIR spectrum of **1** contains seven terminal carbonyl bands between 2066 and 1943 cm^{-1} ; a band at 1864 cm^{-1} , characteristic of edge-bridging carbonyl, is also present. The ^1H NMR spectrum exhibits an ABCD pattern of resonances, suggesting the presence of an orthometallated C_6H_4 ring. The ^{31}P NMR spectrum contains a singlet at 309.6 ppm, characteristic of a phosphido ligand. The FAB mass spectrum has peaks corresponding to the parent ion (at 1262 mass units) and loss of nine successive CO ligands.

Similarly, thermolysis of $[\text{CpWIr}_3(\mu\text{-CO})_3(\text{CO})_6(\text{PPh}_3)_2]$ in toluene for 15 min afforded two major products on workup by preparative thin-layer chromatography. One product was characterized as $[\text{CpWIr}_3\{\mu_3\text{-}\eta^2\text{-PPh}(\text{C}_6\text{H}_4)\}(\mu\text{-CO})_2(\text{CO})_7]$ (**1**) in 23% yield. The other major product was isolated in 39%



Scheme 1. Fragmentation pathway for PRPh_2 on triosmium clusters.

yield as brown crystals of $[\text{CpWIr}_3(\mu_3\text{-}\eta^2\text{-PPh}(\text{C}_6\text{H}_4))\text{-}(\mu\text{-CO})_2(\text{CO})_6(\text{PPh}_3)]$ (**3**), and characterized by a combination of FTIR, ^1H NMR, ^{13}C NMR and ^{31}P NMR spectroscopies and FAB MS. The solution FTIR spectrum contains five terminal carbonyl bands between 2046 and 1963 cm^{-1} . A weak intensity absorption at 1814 cm^{-1} suggests the presence of edge-bridging carbonyls. The ^1H NMR spectrum features an ABCD pattern of signals in the aromatic region, consistent with the presence of an orthometallated C_6H_4 ring, as well as resonances in the expected regions indicating the presence of phenyl and cyclopentadienyl groups. The FAB mass spectrum contains the parent ion at 1496 mass units and sequential loss of seven CO ligands.

In an analogous fashion, heating $[\text{CpWIr}_3(\mu\text{-CO})_3(\text{CO})_5(\text{PPh}_3)_3]$ gave **1** (15%) and **3** (44%). The X-ray structural studies of **1** and **3** were carried out to confirm the identities of the orthometallated products, and to determine the coordination sites of the phosphine ligand (**3**) and phosphido species (**1** and **3**).

2.2. X-ray structural studies of **1** and **3**

Single crystal structural determinations of **1** and **3** were performed; crystallographic data are summarized in Table 1, non-hydrogen positional and equivalent isotropic displacement parameters are listed in Tables 2 (**1**) and 3 (**3**), significant bond lengths are collected in Table 4, and important angles displayed in Table 5. Figs. 1 (**1**) and 2 (**3**) contain plots of the molecular geometries and show the atomic numbering scheme.

Table 1
Crystallographic data for **1** and **3**

	1	3 ^a
Chemical formula	$\text{C}_{26}\text{H}_{14}\text{Ir}_3\text{O}_9\text{PW}$	$\text{C}_{43}\text{H}_{29}\text{Ir}_3\text{O}_8\text{P}_2\text{W} \cdot 0.68\text{CH}_2\text{Cl}_2$
Formula weight	1261.8	1552.4
Space group	$P2_1/c$ (No. 14)	$P\bar{1}$ (No. 2)
Crystal system	Monoclinic	Triclinic
a (Å)	9.612(2)	16.623(10)
b (Å)	26.828(10)	11.919(4)
c (Å)	12.822(3)	11.461(10)
α (deg)		82.66(6)
β (deg)	121.39(2)	79.00(6)
γ (deg)		74.59(4)
V (Å ³)	2822	2142
ρ_{calc} (g cm ⁻³)	2.97	2.41
Z	4	2
μ (mm ⁻¹)	18.3	12.2
Specimen size (mm ³)	0.088 × 0.44 × 0.340	0.23 × 0.11 × 0.18
A^* (min, max)	4.3, 47.2	3.3, 6.6
$2\theta_{\text{max}}$ (deg)	50	55
N	4594	9812
N_{o}	3455	7248
R	0.046	0.046
R_w	0.046	0.051

^a For **3**, difference map residues were modelled as (ordered) CH_2Cl_2 , site occupancy set at 0.68(1) on the basis of refinement.

Table 2

Non-hydrogen atom coordinates and equivalent isotropic displacement parameters for complex **1**

Atom	x	y	z	U_{eq} Å ²
Ir(1)	0.3334(1)	0.42043(2)	0.80293(6)	0.0368(3)
Ir(2)	0.2821(1)	0.32348(3)	0.72413(6)	0.0369(4)
Ir(3)	0.1266(1)	0.36206(3)	0.82755(6)	0.0388(3)
W(4)	0.4749(1)	0.34292(3)	0.97493(6)	0.0422(4)
C(2)	0.354(3)	0.2774(8)	0.890(2)	0.06(1)
O(2)	0.326(2)	0.2354(5)	0.896(1)	0.075(9)
C(3)	0.430(2)	0.4158(7)	1.002(2)	0.044(9)
O(3)	0.443(2)	0.4482(5)	1.072(1)	0.071(9)
C(11)	0.514(3)	0.4442(7)	0.790(2)	0.05(1)
O(11)	0.619(2)	0.4575(7)	0.785(2)	0.10(1)
C(12)	0.246(3)	0.4794(9)	0.808(2)	0.08(1)
O(12)	0.185(3)	0.5170(6)	0.813(2)	0.10(1)
C(21)	0.440(3)	0.3085(8)	0.686(2)	0.054(9)
O(21)	0.542(2)	0.2978(7)	0.666(1)	0.09(1)
C(22)	0.129(2)	0.2740(8)	0.638(2)	0.05(1)
O(22)	0.033(2)	0.2442(7)	0.588(2)	0.10(1)
C(31)	0.018(3)	0.3043(9)	0.830(2)	0.06(1)
O(31)	-0.049(2)	0.2698(7)	0.829(1)	0.10(1)
C(32)	0.069(3)	0.4081(9)	0.911(2)	0.07(1)
O(32)	0.026(3)	0.4348(7)	0.957(2)	0.11(1)
C(41)	0.360(2)	0.3307(7)	1.066(2)	0.05(1)
O(41)	0.324(2)	0.3226(7)	1.134(1)	0.09(1)
P(1)	0.1626(7)	0.3928(2)	0.6085(4)	0.042(2)
C(111)	-0.050(3)	0.3971(7)	0.562(2)	0.05(1)
C(112)	-0.077(3)	0.3829(8)	0.656(2)	0.05(1)
C(113)	-0.234(3)	0.3833(9)	0.629(2)	0.07(1)
C(114)	-0.359(3)	0.394(1)	0.515(2)	0.09(1)
C(115)	-0.332(3)	0.407(1)	0.422(2)	0.09(1)
C(116)	-0.177(3)	0.4100(8)	0.446(2)	0.06(1)
C(121)	0.181(2)	0.4107(7)	0.478(1)	0.04(1)
C(122)	0.159(3)	0.3748(7)	0.394(2)	0.05(1)
C(123)	0.169(3)	0.3876(9)	0.295(2)	0.07(1)
C(124)	0.200(3)	0.436(1)	0.279(2)	0.08(1)
C(125)	0.222(4)	0.4714(9)	0.362(2)	0.08(2)
C(126)	0.215(3)	0.4584(8)	0.467(2)	0.07(2)
C(01)	0.701(4)	0.315(1)	1.151(2)	0.09(2)
C(02)	0.733(4)	0.362(1)	1.138(3)	0.10(2)
C(03)	0.732(3)	0.369(1)	1.035(3)	0.08(1)
C(04)	0.720(3)	0.319(1)	0.988(2)	0.10(2)
C(05)	0.686(3)	0.2870(8)	1.063(3)	0.08(1)

Complexes **1** and **3** have the WIr_3 pseudotetrahedral framework of the precursor clusters $[\text{CpWIr}_3(\mu\text{-CO})_3(\text{CO})_{8-n}(\text{PPh}_3)_n]$ ($n = 1$ to 3) and possess η^5 -cyclopentadienyl groups, two bridging carbonyls spanning W-Ir vectors, seven (**1**) or six (**3**) terminal carbonyl ligands, a triphenylphosphine ligand (**3**), and a $\mu_3\text{-}\eta^2$ -bound orthometallated phosphido moiety capping the triiridium planes. The WIr_3 core distances in **1** and **3** are inequivalent, with the longest (2.907(1) Å (**1**), 2.880(1) Å (**3**)) being those not bearing a bridging carbonyl ligand; as with other phosphine-substituted tungsten-iridium clusters, the longest W-Ir vectors are those effectively *trans* to the cyclopentadienyl groups [7]. The bridging carbonyl ligands in **1** and **3** bridge asymmetrically; in **1**, both ligands are displaced toward the tungsten, whereas in **3**, CO(3) is closer to Ir(1). The

Table 3
Non-hydrogen atom coordinates and equivalent isotropic displacement parameters for complex **3**

Atom	<i>x</i>	<i>y</i>	<i>z</i>	U_{eq} Å ²
Ir(1)	0.19267(3)	0.85769(4)	0.16304(5)	0.0293(2)
Ir(2)	0.30886(3)	0.98883(4)	0.13619(5)	0.0308(2)
Ir(3)	0.27872(3)	0.86334(4)	0.34085(5)	0.0324(2)
W(4)	0.15141(3)	1.06731(4)	0.27881(5)	0.0357(2)
C(2)	0.256(1)	1.132(1)	0.272(1)	0.052(6)
O(2)	0.2917(7)	1.1958(9)	0.292(1)	0.068(5)
C(3)	0.1085(9)	0.905(1)	0.315(1)	0.044(5)
O(3)	0.0602(6)	0.8650(8)	0.3874(9)	0.054(4)
C(11)	0.1374(9)	0.911(1)	0.031(1)	0.043(5)
O(11)	0.1042(7)	0.9459(9)	-0.049(1)	0.064(5)
C(21)	0.2973(8)	1.077(1)	-0.009(1)	0.048(6)
O(21)	0.2904(8)	1.130(1)	-0.100(1)	0.081(6)
C(22)	0.425(1)	0.986(1)	0.147(1)	0.046(6)
O(22)	0.4915(7)	0.977(1)	0.146(1)	0.070(5)
C(31)	0.351(1)	0.922(1)	0.408(1)	0.046(6)
O(31)	0.4028(9)	0.952(1)	0.439(1)	0.086(7)
C(32)	0.231(1)	0.782(1)	0.475(1)	0.049(6)
O(32)	0.2014(8)	0.734(1)	0.560(1)	0.074(5)
C(41)	0.1517(8)	1.039(1)	0.443(2)	0.048(6)
O(41)	0.1410(7)	1.034(1)	0.551(1)	0.069(5)
P(1)	0.3330(2)	0.8058(3)	0.0755(3)	0.033(1)
C(111)	0.3981(8)	0.696(1)	0.167(1)	0.033(4)
C(112)	0.3774(8)	0.718(1)	0.289(1)	0.039(5)
C(113)	0.4227(9)	0.638(1)	0.366(1)	0.047(6)
C(114)	0.484(1)	0.543(1)	0.325(2)	0.055(6)
C(115)	0.5024(9)	0.522(1)	0.209(1)	0.049(6)
C(116)	0.4594(8)	0.599(1)	0.126(1)	0.039(5)
C(121)	0.3798(8)	0.788(1)	-0.077(1)	0.036(5)
C(122)	0.4671(9)	0.774(1)	-0.115(1)	0.044(5)
C(123)	0.502(1)	0.771(1)	-0.231(2)	0.056(6)
C(124)	0.452(1)	0.781(2)	-0.318(2)	0.066(7)
C(125)	0.366(1)	0.796(2)	-0.284(2)	0.071(8)
C(126)	0.3306(9)	0.799(1)	-0.164(1)	0.048(6)
P(2)	0.1582(2)	0.6776(3)	0.1849(3)	0.036(1)
C(211)	0.1752(8)	0.588(1)	0.324(1)	0.043(5)
C(212)	0.254(1)	0.533(1)	0.346(1)	0.054(6)
C(213)	0.265(1)	0.463(2)	0.451(2)	0.09(1)
C(214)	0.196(1)	0.449(2)	0.536(2)	0.082(9)
C(215)	0.117(1)	0.508(2)	0.512(2)	0.075(9)
C(216)	0.106(1)	0.573(1)	0.409(1)	0.057(7)
C(221)	0.211(1)	0.584(1)	0.065(2)	0.058(7)
C(222)	0.267(1)	0.475(2)	0.082(2)	0.09(1)
C(223)	0.303(1)	0.410(2)	-0.018(3)	0.12(1)
C(224)	0.285(2)	0.453(3)	-0.130(3)	0.13(2)
C(225)	0.234(2)	0.559(2)	-0.144(2)	0.10(1)
C(226)	0.197(1)	0.625(2)	-0.050(2)	0.079(9)
C(231)	0.0490(8)	0.683(1)	0.177(1)	0.040(5)
C(232)	-0.0157(9)	0.785(1)	0.190(1)	0.050(6)
C(233)	-0.0979(9)	0.780(1)	0.187(2)	0.062(7)
C(234)	-0.115(1)	0.681(2)	0.166(2)	0.064(7)
C(235)	-0.053(1)	0.583(2)	0.151(2)	0.066(8)
C(236)	0.030(1)	0.581(1)	0.156(2)	0.055(6)
C(01)	0.026(1)	1.201(2)	0.343(2)	0.077(8)
C(02)	0.010(1)	1.142(2)	0.254(3)	0.09(1)
C(03)	0.059(1)	1.170(2)	0.147(2)	0.078(9)
C(04)	0.102(1)	1.242(1)	0.168(2)	0.063(7)
C(05)	0.083(1)	1.262(1)	0.286(2)	0.074(9)
C1(1) *	0.5879(5)	0.7537(7)	0.3534(8)	0.096(4)
C1(2) *	0.7127(5)	0.8668(9)	0.3860(9)	0.114(5)
C(0) *	0.612(2)	0.871(3)	0.377(3)	0.10(2)

* Site occupancy factor 0.68(1).

latter presumably results from ligation of triphenylphosphine at Ir(1), and the consequent increase in electron density at this metal. Distances and angles involving the phosphines are not unusual. Those involving the terminal carbonyl ligands are relatively imprecise; the most dramatic difference between **1** and **3** is in the geometry about CO(4) [W(4)–C(41) 2.01(3) Å (**1**), 1.87(2) Å (**3**)], with the shorter bond in **3** possibly a result of compensation for the asymmetry of CO(3). The (phenylphosphido)phenyl-*P,C* ligands cap the triiridium faces. The phosphido *P* bridges an Ir–Ir vector symmetrically in both **1** and **3**; the corresponding WIr₂ face thus has bridging ligands about all edges, and it is over this face that the cyclopentadienyl ligands sit. The orthometalated phenyl interacts with the remaining iridium. Electron counting procedures reveal that both **1** and **3** have 60 CVE, electron precise for clusters possessing tetrahedral cores.

Crystallographically-verified clusters containing orthometalated diphenylphosphido ligands are comparatively rare; there are no precedents in the tetrairidium system for clusters of this type, with previous examples being confined to the iron subgroup [3c,8], and a mixed ruthenium–iridium cluster [Ru₃Ir(μ-H)₂(μ₃-η²-PPh-C₆H₄)(μ-PPh₂)(μ-CO)(CO)₇(PPh₃)] (**4**) [9]. In the ruthenium–iridium cluster **4**, the PPhC₆H₄ group face-caps at an Ru₂Ir face with the phosphorus bridging an Ru–Ru bond and the orthometalated phenyl group bound to the iridium. Cluster **1** is also metallated at iridium; this is perhaps understandable in the present work owing to the enhanced carbophilicity of iridium compared with tungsten. The Ir–C(*ortho*) linkage is shorter in **4** than in **1** or **3** (2.086(7) Å (**4**) vs. 2.12(2) Å (**1**), 2.11(1) Å (**3**)), although differences are within error margins. The phosphine ligates at the orthometalated phenyl-bound iridium in **4**, unlike in **3**, where it coordinates to a phosphido-bound iridium. Phosphido bridges in the tetrairidium system are rare; in [Ir₄(μ-H)(μ-PPh₂)(μ-CO)(CO)₈(PPh₃)] (**5**), the phosphido bridges symmetrically, with Ir–P_{av} 2.30 Å similar to the corresponding distances in **1** and **3** [10]. In contrast to **3**, cluster **5** contains a phosphine ligand at a non-phosphido-ligated iridium.

2.3. Discussion

The results of the thermolytic investigations detailed above are summarized in Scheme 2. All three reactions proceed to give a mixture of products, with the identified components of the reaction mixtures accounting for 60–90% of the theoretical yields. Thermolyses in the related triosmium system proceed by initial loss of CO to generate a vacant coordination site, and subsequent oxidative addition of a phenyl *ortho*-C–H bond across the Os–Os bond. Subsequent loss of CO, rearrange-

Table 4
Important bond lengths (Å) for complexes 1 and 3

	1	3		1	3
Ir(1)–Ir(2)	2.741(1)	2.743(1)	Ir(1)–Ir(3)	2.676(1)	2.721(2)
Ir(1)–W(4)	2.813(1)	2.839(1)	Ir(2)–Ir(3)	2.670(2)	2.654(2)
Ir(2)–W(4)	2.800(1)	2.803(1)	Ir(3)–W(4)	2.907(1)	2.880(1)
W(4)–C(01)	2.30(2)	2.32(2)	W(4)–C(02)	2.32(2)	2.33(2)
W(4)–C(03)	2.28(3)	2.36(2)	W(4)–C(04)	2.36(3)	2.33(2)
W(4)–C(05)	2.29(2)	2.30(1)	Ir(1)–P(1)	2.279(4)	2.308(3)
Ir(2)–P(1)	2.281(5)	2.285(3)	Ir(1)–P(2)		2.337(4)
Ir(2)–C(2)	2.24(2)	2.34(2)	Ir(1)–C(3)	2.22(2)	2.05(1)
W(4)–C(2)	2.07(2)	2.06(2)	W(4)–C(3)	2.07(2)	2.20(1)
C(2)–O(2)	1.17(3)	1.15(2)	C(3)–O(3)	1.21(3)	1.19(2)
C(01)–C(02)	1.32(4)	1.42(4)	C(02)–C(03)	1.34(5)	1.39(3)
C(03)–C(04)	1.45(5)	1.32(3)	C(04)–C(05)	1.45(5)	1.37(3)
C(01)–C(05)	1.30(4)	1.36(3)	P(1)–C(111)	1.81(3)	1.82(1)
P(1)–C(121)	1.83(2)	1.78(1)	P(2)–C(211)		1.83(1)
P(2)–C(221)		1.82(2)	P(2)–C(231)		1.82(1)
Ir(3)–C(112)	2.12(2)	2.11(1)	C(111)–C(112)	1.42(4)	1.41(2)
Ir(1)–C(11)	1.93(3)	1.87(2)	Ir(1)–C(12)	1.81(3)	
Ir(2)–C(21)	1.87(3)	1.86(2)	Ir(2)–C(22)	1.86(2)	1.94(2)
Ir(3)–C(31)	1.88(3)	1.85(2)	Ir(3)–C(32)	1.89(3)	1.87(1)
W(4)–C(41)	2.01(3)	1.87(2)	C(11)–O(11)	1.10(4)	1.14(2)
C(12)–O(12)	1.18(3)		C(21)–O(21)	1.17(4)	1.16(2)
C(22)–O(22)	1.13(3)	1.09(2)	C(31)–O(31)	1.12(3)	1.15(2)
C(32)–O(32)	1.14(4)	1.16(2)	C(41)–O(41)	1.11(3)	1.22(2)

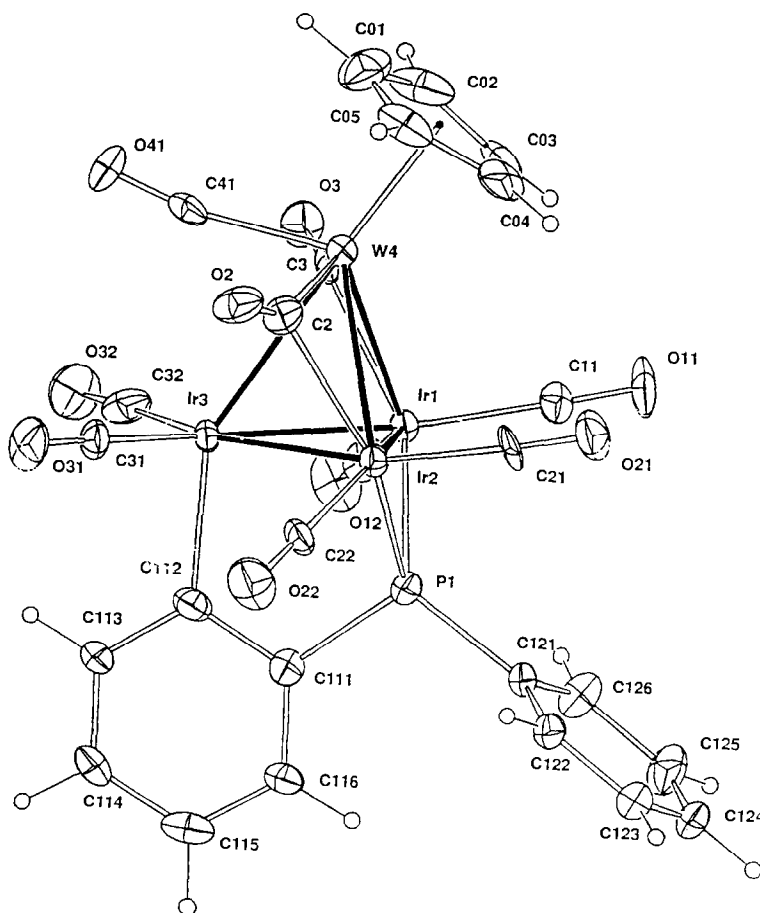


Fig. 1. Molecular structure and atomic labelling scheme for $[\text{CpWIr}_3\{\mu_3\text{-}\eta^2\text{-PPh}(\text{C}_6\text{H}_4)\}(\mu\text{-CO})_2(\text{CO})_7]$ 1. 20% thermal envelopes are shown for the non-hydrogen atoms; hydrogen atoms have arbitrary radii of 0.1 Å.

ment, addition of CO and loss of benzene form triosmium complexes bearing orthometallated ligands analogous to those in **1** and **3** (Scheme 1). While a similar process may be operative in the tungsten–iridium system in the conversion of $[\text{CpWIr}_3(\mu\text{-CO})_3(\text{CO})_7(\text{PPh}_3)]$ into **1** and $[\text{CpWIr}_3(\mu\text{-CO})_3(\text{CO})_6(\text{PPh}_3)_2]$ into **3**, the mixtures of products suggest that other pathways are accessible; the transformation of $[\text{CpWIr}_3(\mu\text{-CO})_3(\text{CO})_7(\text{PPh}_3)]$ into $[\text{CpWIr}_3(\text{CO})_{11}]$, and $[\text{CpWIr}_3(\mu\text{-CO})_3(\text{CO})_6(\text{PPh}_3)_2]$ into **1**, and the formation of **1** and **3** from heating $[\text{CpWIr}_3(\mu\text{-CO})_3(\text{CO})_5(\text{PPh}_3)_3]$, is consistent with the loss of PPh_3 being competitive with loss of CO for the system under investigation. The product distributions also suggest that this pathway becomes increasingly important on proceeding from $[\text{CpWIr}_3(\mu\text{-CO})_3(\text{CO})_7(\text{PPh}_3)]$ through $[\text{CpWIr}_3(\mu\text{-CO})_3(\text{CO})_6(\text{PPh}_3)_2]$ to $[\text{CpWIr}_3(\mu\text{-CO})_3(\text{CO})_5(\text{PPh}_3)_3]$. Indeed, for the last mentioned cluster, initial loss of PPh_3 seems specific, chemistry which is mirrored in its FAB MS where $[\text{M-PPh}_3]^+$ rather than $[\text{M}]^+$ is observed, and in its solution chemistry, where it slowly transforms into $[\text{CpWIr}_3(\mu\text{-CO})_3(\text{CO})_6(\text{PPh}_3)_2]$ at room temperature over days [1].

The relatively good yield of the orthometallated product **1** prompted us to examine its derivative chem-

istry, in a bid to generate benzyne fragments on a mixed-metal cluster, analogous to those described previously for homometallic systems; clusters of type **1** react to form benzyne derivatives by way of decarbonylation (Scheme 1), so attempted elimination of CO was pursued. All rational attempts proved fruitless, however, with thermolysis, photolysis, and the attempted generation of a vacant coordination site by employing trimethylamine-*N*-oxide all affording intractable mixtures. Attempted functionalization utilizing diphenylacetylene was also unsuccessful.

It is well known that P–C(aryl) cleavage is favoured over P–C(methyl). However, double C–H activation of coordinated trimethylphosphine has been achieved in converting $[\text{Os}_3(\text{CO})_{11}(\text{PMe}_3)]$ into $[\text{Os}_3(\mu\text{-H})_2(\mu_3\text{-}\eta^2\text{-Me}_2\text{PCH}(\text{CO})_9)]$ [4c]. This pathway does not seem accessible in the tungsten–iridium system; heating $[\text{CpWIr}_3(\mu\text{-CO})_3(\text{CO})_7(\text{PMe}_3)]$ (refluxing tetrahydrofuran, 15 min) does not lead to any tractable products.

We have shown in earlier work that (conceptual) isolobal replacement of one $\text{Ir}(\text{CO})_3$ vertex in $[\text{Ir}_4(\text{CO})_{12}]$ by $\text{CpW}(\text{CO})_2$ to give $[\text{CpWIr}_3(\text{CO})_{11}]$ facilitates phosphine substitution at iridium; whereas reaction of $[\text{Ir}_4(\text{CO})_{12}]$ with phosphine requires forcing conditions (heating at 80–110 °C) [11] to proceed, phosphines

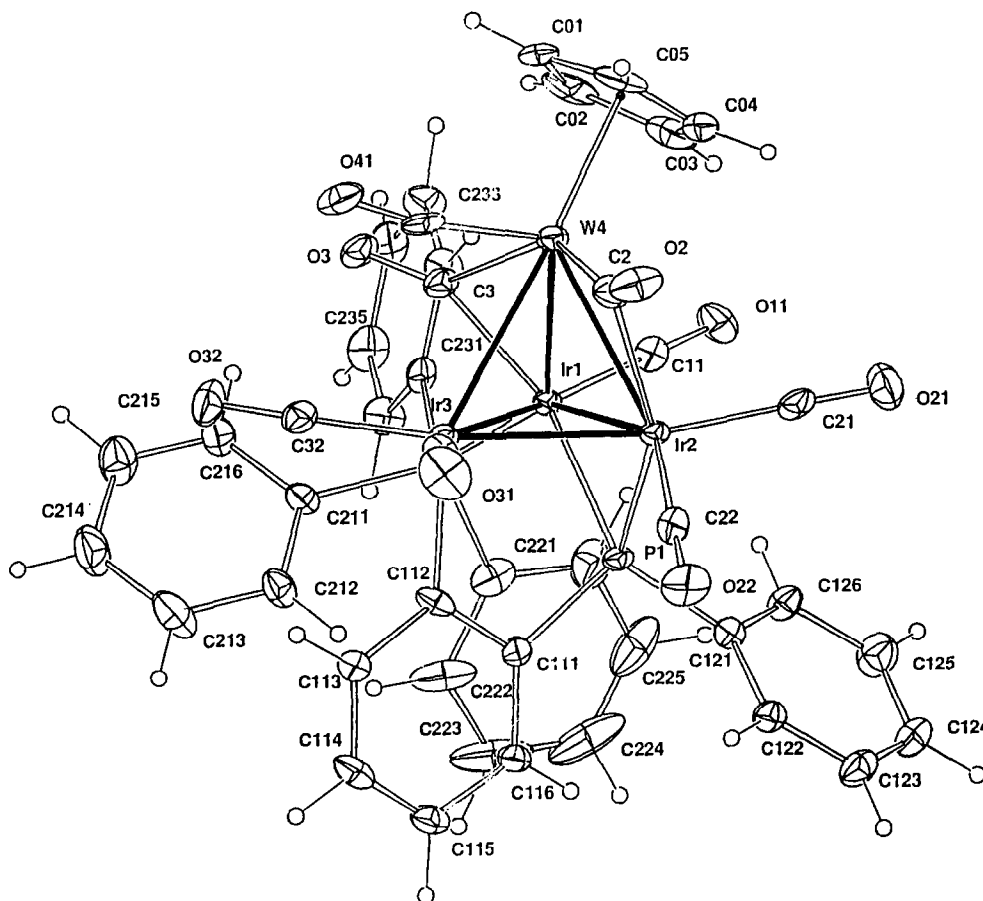


Fig. 2. Molecular structure and atomic labelling scheme for $[\text{CpWIr}_3(\mu_3\text{-}\eta^2\text{-PPh}(\text{C}_6\text{H}_4))(\mu\text{-CO})_2(\text{CO})_6(\text{PPh}_3)]$ **3**. 20% thermal envelopes are shown for the non-hydrogen atoms; hydrogen atoms have arbitrary radii of 0.1 Å.

Table 5
Selected bond angles (deg) for complexes **1** and **3**

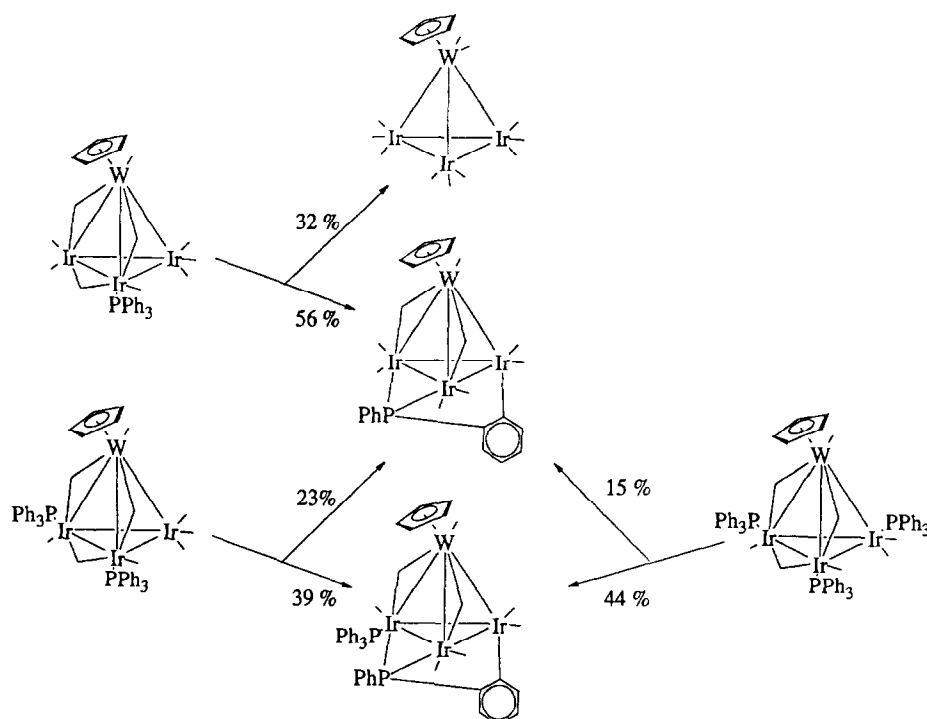
	1	3
Ir(2)–Ir(1)–Ir(3)	59.06(3)	58.12(4)
Ir(2)–Ir(1)–W(4)	60.53(3)	60.24(3)
Ir(3)–Ir(1)–W(4)	63.91(3)	62.34(3)
Ir(1)–Ir(2)–Ir(3)	59.26(4)	60.52(3)
Ir(3)–Ir(2)–W(4)	64.17(4)	63.64(4)
Ir(1)–Ir(3)–Ir(2)	61.68(4)	61.36(5)
Ir(1)–Ir(3)–W(4)	60.34(3)	60.85(3)
Ir(2)–Ir(3)–W(4)	60.09(3)	60.69(3)
Ir(1)–W(4)–Ir(2)	58.45(3)	58.17(3)
Ir(1)–W(4)–Ir(3)	55.75(3)	56.81(4)
Ir(2)–W(4)–Ir(3)	55.75(3)	55.67(4)
Ir(2)–C(2)–W(4)	80.8(8)	78.9(6)
Ir(2)–C(2)–O(2)	128(1)	125(1)
W(4)–C(2)–O(2)	150(1)	156(1)
Ir(1)–C(3)–W(4)	82.0(7)	83.9(5)
Ir(1)–C(3)–O(3)	129(1)	138(1)
W(4)–C(3)–O(3)	148(1)	138(1)
W(4)–C(41)–O(41)	167(2)	170(1)
Ir(1)–P(1)–Ir(2)	73.9(1)	73.33(9)
Ir(1)–Ir(2)–P(1)	53.0(1)	53.73(8)
Ir(2)–Ir(1)–P(1)	53.1(1)	52.94(9)
Ir(1)–P(1)–C(111)	112.7(7)	112.9(4)
Ir(2)–P(1)–C(111)	111.5(7)	111.8(5)
P(1)–C(111)–C(112)	113(1)	112.3(8)
Ir(3)–C(112)–C(111)	118(2)	118.5(9)
Ir(1)–Ir(3)–C(112)	93.8(7)	94.1(4)
Ir(2)–Ir(3)–C(112)	92.4(7)	93.6(4)

react with $[\text{CpWIr}_3(\text{CO})_{11}]$ at room temperature. Differences in reactivity extend to thermolyses, with the mixed tungsten–iridium system affording examples of

orthometallation of the phenylphosphine-substituted clusters, cluster system types not thus far identified in the tetrairidium system (it has been reported that, in contrast to the triosmium system, thermolysis of $[\text{Ir}_4(\mu\text{-H})(\mu\text{-PPh}_2)(\mu\text{-CO})(\text{CO})_8(\text{PPh}_3)]$ (**5**) does not afford orthometallated products). Our comparisons of the reactivity of these related cluster systems are proceeding; further examples will be reported shortly.

3. Experimental details

All reactions were performed under an atmosphere of dry nitrogen (high purity grade, CIG), although no special precautions were taken to exclude air during workup. The reaction solvents dichloromethane (CaH_2), acetonitrile (CaH_2) and toluene (sodium/benzophenone) were dried and distilled under argon before use. All other solvents were reagent grade, and used as received. Petroleum ether refers to a fraction of boiling point range 60–70 °C. The progress of reactions was monitored by analytical thin-layer chromatography (5554 Kieselgel 60 PF_{254} , E. Merck), and the products were separated on $20 \times 20 \text{ cm}^2$ glass plates coated with 7749 Kieselgel 60 PF_{254} (E. Merck). Diphenylacetylene was purchased commercially (Aldrich) and used as received. Trimethylamine-*N*-oxide dihydrate was purchased commercially (Aldrich) and sublimed before use. The clusters $[\text{CpWIr}_3(\mu\text{-CO})_3(\text{CO})_7(\text{PPh}_3)]$ [**7**], $[\text{CpWIr}_3(\mu\text{-CO})_3(\text{CO})_6(\text{PPh}_3)_2]$ [**1**], $[\text{CpWIr}_3(\mu\text{-CO})_3-$



Scheme 2. Thermolyses of $[\text{CpWIr}_3(\text{CO})_{11-n}(\text{PPh}_3)_n]$ ($n = 1, 2$ or 3). Reaction conditions: toluene, 110°C, 15 min.

(CO)₅(PPh₃)₃] [1], and [CpWIr₃(μ-CO)₃(CO)₇(PMe₃)₃] [1] were prepared by the published procedures.

Infrared spectra were recorded on a Perkin-Elmer 1600 FTIR spectrometer using CaF₂ optics. ¹H and ¹³C NMR spectra were recorded on a Bruker AC300 FT spectrometer (¹H NMR at 300 MHz, ¹³C NMR at 75 MHz). All ¹³C NMR spectra were obtained by spectral addition of blocks of 6000 acquisitions; the samples contained ca. 0.02 M Cr(acac)₃ and utilized a 0.5 s recycle delay. The ³¹P NMR spectra were recorded on a Varian Gemini 300 spectrometer. All NMR spectra were run in CDCl₃ (Aldrich); chemical shifts in ppm are referenced to internal residual solvent for ¹H and ¹³C NMR spectra and external H₃PO₄ for ³¹P NMR spectra.

Fast atom bombardment (FAB) mass spectra were obtained at the University of Adelaide on a VG ZAB 2HF mass spectrometer (FAB source of argon at 10⁻⁶ mbar, FAB gun voltage 7.5 kV, current 1 mA, ion accelerating potential 8 kV, matrix 3-nitrobenzyl alcohol, ca. 0.5 M solutions in dichloromethane). All FAB MS were calculated with *m/z* based on ¹⁸³W assignments and are reported in the form: *m/z* (assignment, relative intensity). Elemental microanalyses were performed by the Microanalysis Service Unit in the Department of Chemistry, University of Queensland. Decomposition temperatures and melting points were measured in sealed capillaries using a Gallenkamp melting point apparatus.

3.1. Thermolysis of [CpWIr₃(μ-CO)₃(CO)₇(PPh₃)₃]

An orange solution of [CpWIr₃(μ-CO)₃(CO)₇(PPh₃)₃] (20.0 mg, 0.0146 mmol) in toluene (15 ml) was slowly heated to 110 °C and refluxed for 15 min. The dark red solution obtained was evaporated to dryness. The deep red residue was then redissolved in CH₂Cl₂ (ca. 1 ml) and chromatographed (1 CH₂Cl₂: 2 petroleum ether eluant) to afford two products. The contents of the major purple band, *R_f* 0.40, were crystallized (CHCl₃/MeOH) to afford purple crystals of [CpWIr₃{μ₃-η²-PPh(C₆H₄)}(μ-CO)₂(CO)₇], **1** (12.2 mg, 56%, m.p. 121 °C (dec.)). **1**: IR (c-C₆H₁₂) 2065m, 2042s, 2030m, 2003s, 1995m, 1978w, 1943w, 1864w cm⁻¹; ¹H NMR (CDCl₃) δ 7.55 (m, 5H, Ph), 7.37 (m, 1H, C₆H₄), 6.91 (t, *J*_{HP} = 7 Hz, 1H, C₆H₄), 6.63–6.57 (m, 1H, C₆H₄), 6.15 (t, *J*_{HP} = 7 Hz, 1H, C₆H₄), 5.28 (s, 5H, C₅H₅); ¹³C NMR (CDCl₃) δ 131–127 (Ph), 91.7 (C₅H₅), other signals not detected; ³¹P NMR (CDCl₃) δ 309.6; FAB MS 1262 ([M]⁺, 30), 1234 ([M-CO]⁺, 44), 1206 ([M-2CO]⁺, 18), 1178 ([M-3CO]⁺, 100), 1150 ([M-4CO]⁺, 22), 1122 ([M-5CO]⁺, 26), 1094 ([M-6CO]⁺, 54), 1066 ([M-7CO]⁺, 47), 1038 ([M-8CO]⁺, 45), 1010 ([M-9CO]⁺, 32). Anal. Found: C, 24.50; H, 1.02. C₂₆H₁₄Ir₃O₉PW Calc.: C, 24.75; H, 1.12%.

The minor product, *R_f* 0.60, was recrystallized from CH₂Cl₂/MeOH to afford orange crystals of

[CpWIr₃(CO)₁₁], **2** (5.3 mg, 32%, m.p. 158 °C (dec.)). **2**: IR (c-C₆H₁₂) 2091m, 2054vs, 2049vs, 2029s, 1997m, 1981m, 1964w cm⁻¹ (cf. lit. 2093m, 2053vs, 2049vs, 2031vs, 1996m, 1979m, 1967w [12]).

3.2. Thermolysis of [CpWIr₃(μ-CO)₃(CO)₆(PPh₃)₂]

An orange solution of [CpWIr₃(μ-CO)₃(CO)₆(PPh₃)₂] (20.0 mg, 0.0125 mmol) in toluene (20 ml) was heated to 110 °C and refluxed for 15 min. Solvent was removed in vacuo from the resulting brown solution. Subsequent purification by thin-layer chromatography (1 CH₂Cl₂: 1 petroleum ether eluant) afforded five bands, of which all but bands 2 and 5 were present in trace amounts. The contents of band 2, *R_f* 0.40, were crystallized from CHCl₃/MeOH to give purple crystals of [CpWIr₃{μ₃-η²-PPh(C₆H₄)}(μ-CO)₂(CO)₇], **1** (3.6 mg, 23%), identified by IR spectroscopy. The contents of band 5, *R_f* 0.25, were crystallized from CH₂Cl₂/MeOH to afford [CpWIr₃{μ₃-η²-PPh(C₆H₄)}(μ-CO)₂(CO)₆(PPh₃)], **3** (7.3 mg, 39%, m.p. 125 °C (dec.)). **3**: IR (c-C₆H₁₂) 2046s, 2025vs, 1998m, 1984m, 1963vw, 1899w, 1814vw cm⁻¹; ¹H NMR (CDCl₃) δ 7.32–7.12 (s, 20H, Ph), 7.00 (t, *J*_{HP} = 7 Hz, 1H, C₆H₄), 6.82–6.71 (m, 2H, C₆H₄), 6.18 (t, *J*_{HP} = 7 Hz, 1H, C₆H₄), 5.38 (s, 5H, C₅H₅), 5.32 (s, 1.3H, CH₂Cl₂); ¹³C NMR (CDCl₃) δ 222.0 (s, μ-CO), 178.7 (s, CO), 172.2 (s, CO), 170.7 (s, CO), 169.7 (s, C112, C₆H₄), 162.3 (s, CO), 143.9 (d, *J*_{CP} = 18 Hz, C111, C₆H₄), 135.7 (d, *J*_{CP} = 40 Hz, *i*-C, PPh₃), 135.7 (d, *J*_{CP} = 35 Hz, *i*-C, Ph), 133.9 (d, *J*_{CP} = 11 Hz, *m*-C, PPh₃), 130.2 (s, *p*-C, PPh₃), 129.7 (s, *p*-C, Ph), 129.4 (d, *J*_{CP} = 12 Hz, *m*-C, Ph), 128.3 (d, *J*_{CP} = 9 Hz, *o*-C, Ph), 128.1 (d, *J*_{CP} = 11 Hz, *o*-C, PPh₃), 127.3 (d, *J*_{CP} = 11 Hz, C116, C₆H₄), 122.3 (d, *J*_{CP} = 7.5 Hz, C115, C₆H₄), 91.5 (s, C₅H₅), 53.8 (s, CH₂Cl₂), C113, C114 not assigned; ³¹P NMR (CDCl₃) δ 267.5 (s, 1P, PPhC₆H₄), 7.9 (s, 1P, PPh₃); FAB MS 1496 ([M]⁺, 24), 1468 ([M-1CO]⁺, 9), 1440 ([M-2CO]⁺, 12), 1412 ([M-3CO]⁺, 21), 1384 ([M-4CO]⁺, 100), 1356 ([M-5CO]⁺, 72), 1328 ([M-6CO]⁺, 24). Anal. Found: C, 34.03; H, 1.84. C₄₃H₂₉Ir₃O₈P₂W.0.68CH₂Cl₂ Calc.: C, 33.95; H, 1.96%.

3.3. Thermolysis of [CpWIr₃(μ-CO)₃(CO)₅(PPh₃)₃]

An orange solution of [CpWIr₃(μ-CO)₃(CO)₅(PPh₃)₃] (25.2 mg, 0.0137 mmol) in toluene (15 ml) was slowly heated to 110 °C and refluxed for 15 min. The brown solution obtained was evaporated to dryness. The resultant brown residue was redissolved in CH₂Cl₂ (ca. 1 ml) and purified by thin-layer chromatography (1 CH₂Cl₂: 2 petroleum ether eluant) to afford seven bands. The contents of the second band, *R_f* 0.40, were crystallized from CHCl₃/MeOH and characterized as [CpWIr₃{μ₃-η²-PPh(C₆H₄)}(μ-CO)₂(CO)₇], **1** (2.3 mg,

15%), by IR spectroscopy. The contents of the sixth, and major, band were crystallized from $\text{CHCl}_3/\text{MeOH}$ to give brown crystals of $[\text{CpWIr}_3\{\mu_3\text{-}\eta^2\text{-PPh}(\text{C}_6\text{H}_4)\}(\mu\text{-CO})_2(\text{CO})_6(\text{PPh}_3)]$, **3** (9.0 mg, 44%), characterized by IR spectroscopy. All other bands were present in trace amounts.

3.4. Thermolysis of **1**

A solution of **1** (15.0 mg, 0.0119 mmol) in xylene (15 ml) was slowly heated to 120 °C and stirred for 15 min, at which stage a brown precipitate was evident in the dark reaction mixture. The solvent was removed in vacuo and the residue taken up in dichloromethane (ca. 1 ml). Purification by thin-layer chromatography (1 acetone: 1 petroleum ether) eluted three bands in trace amounts.

3.5. Photolysis of **1**

A solution of **1** (15.0 mg, 0.0119 mmol) in acetonitrile (15 ml) was stirred and irradiated for 45 min with a 450 W mercury-arc lamp. The solvent was removed in vacuo leaving a brown residue. Subsequent purification by thin-layer chromatography (1 CH_2Cl_2 : 1 petroleum ether eluant) gave three bands in trace amounts.

3.6. Reaction of **1** with Me_3NO

A solution of **1** (15.0 mg, 0.0119 mmol) and Me_3NO (0.89 mg, 0.012 mmol) in acetonitrile (15 ml) was stirred for 1 h. The solvent was removed in vacuo, leaving a brown residue. No tractable products were obtained.

3.7. Reaction of **1** with diphenylacetylene

A solution of **1** (2.9 mg, 0.23 μmol) and diphenylacetylene (0.4 mg, 0.23 μmol) in toluene (10 ml) was stirred at room temperature for 18 h. No reaction was observed. The solution was warmed and monitored by IR at 60, 80 and 100 °C, stirring for 1 h at each interval. The solution was finally refluxed for 2 h. The solvent was removed in vacuo, leaving a brown residue. Subsequent purification by thin-layer chromatography (1 CH_2Cl_2 : 1 petroleum ether eluant) afforded one band of starting material.

3.8. Thermolysis of $[\text{CpWIr}_3(\mu\text{-CO})_3(\text{CO})_7(\text{PMe}_3)]$

An orange solution of $[\text{CpWIr}_3(\mu\text{-CO})_3(\text{CO})_7(\text{PMe}_3)]$ (24.7 mg, 0.0201 mmol) in toluene (15 ml) was slowly heated to 110 °C and refluxed for 15 min. No reaction was apparent by IR monitoring of the reaction mixture. The solution was allowed to reflux for a further 45 min. Decomposition of the cluster was observed.

3.9. Structure determinations

Crystals of compounds **1** and **3** suitable for diffraction analyses were grown by slow diffusion of methanol into dichloromethane solutions at room temperature. Unique diffractometer data sets were measured at around 295 K within the specified $2\theta_{\text{max}}$ limit ($2\theta/\theta$ scan mode; monochromatic Mo K α radiation ($\lambda = 0.71073$ Å)) yielding N independent reflections. N_o of these with $I > 3\sigma(I)$ were considered "observed" and used in the full-matrix/large-block least-squares refinements after analytical absorption correction. Anisotropic thermal parameters were refined for the non-hydrogen atoms; (x, y, z, U_{iso})_H were included, constrained at estimated values. Conventional residuals R, R_w on $|F|$ at convergence are given, statistical weights derivative of $\sigma^2(I) = \sigma^2(I_{\text{diff}}) + 0.0004\sigma^4(I_{\text{diff}})$ being used. Neutral atom complex scattering factors were used, with computation by the XTAL 3.2 program system [13] implemented by Hall et al. Pertinent results are given in the figures and tables. Tables of final values of all atomic coordinates and thermal parameters, and a complete list of bond lengths and angles, have been deposited at the Cambridge Crystallographic Data Centre.

Acknowledgements

We thank the Australian Research Council for support of this work and Johnson-Matthey Technology Centre for the loan of IrCl_3 . MGH is an ARC Australian Research Fellow.

References

- [1] S.M. Waterman, M.G. Humphrey, V.-A. Tolhurst, B.W. Skelton and A.H. White, *Organometallics*, in press.
- [2] P.E. Garrou, *Chem. Rev.*, **85** (1985) 171.
- [3] (a) M.I. Bruce, G. Shaw and F.G.A. Stone, *J. Chem. Soc., Dalton Trans.*, (1972) 2094. (b) M.I. Bruce, J.M. Guss, R. Mason, B.W. Skelton and A.H. White, *J. Organomet. Chem.*, **251** (1983) 261. (c) H. Jungbluth, G. Süß-Fink, M.A. Pellinghelli and A. Tiripicchio, *Organometallics*, **8** (1989) 925. (d) S.A.R. Knox, B.R. Lloyd, A.G. Orpen, J.M. Vinas and M. Weber, *J. Chem. Soc., Chem. Commun.*, (1987) 1498.
- [4] (a) C.W. Bradford and R.S. Nyholm, *J. Chem. Soc., Dalton Trans.*, (1973) 529. (b) W.R. Cullen, D. Harborne, B. Leingme and J.R. Sams, *Inorg. Chem.*, **9** (1970) 702. (c) W.R. Cullen, *Adv. Inorg. Chem. Radiochem.*, **15** (1972) 323. (d) A.J. Deeming, R.E. Kimber and M. Underhill, *J. Chem. Soc., Dalton Trans.*, (1973) 2589. (e) A.J. Deeming and M. Underhill, *J. Chem. Soc., Dalton Trans.*, (1973) 2727. (f) G.J. Gainsford, J.M. Guss, P.R. Ireland, R. Mason, C.W. Bradford and R.S. Nyholm, *J. Organomet. Chem.*, **40** (1972) C70. (g) C.W. Bradford, R.S. Nyholm, G.J. Gainsford, J.M. Guss, P.R. Ireland and R. Mason, *J. Chem. Soc., Chem. Commun.*, (1972) 87. (h) C.W. Bradford and R.S. Nyholm, *J. Chem. Soc., Chem. Commun.*, (1972) 2094. (i) A.J. Deeming, I.P. Rothwell, M.B.

- Hursthouse and J.D.J. Backer-Dirks, *J. Chem. Soc., Dalton Trans.*, (1981) 1879. (j) S.C. Brown, J. Evans, and L. Smart, *J. Chem. Soc., Chem. Commun.*, (1980) 1021.
- [5] F. Demartin, M. Manassero and M. Sansoni, *J. Organomet. Chem.*, 204 (1981) C10.
- [6] V.G. Albano, D. Braga, R. Ros and A. Scrivanti, *J. Chem. Soc., Chem. Commun.*, (1985) 866.
- [7] J. Lee, M.G. Humphrey, D.C.R. Hockless, B.W. Skelton and A.H. White, *Organometallics*, 12 (1993) 3468.
- [8] (a) S.B. Colbran, P.T. Irele, B.F.G. Johnson, F.J. Lahoz, J. Lewis and P.R. Raithby, *J. Chem. Soc., Dalton Trans.*, (1989) 2023. (b) J.F. Corrigan, S. Doherty, N.J. Taylor, A.J. Carty, E. Boroni and A. Tiripicchio, *J. Organomet. Chem.*, 462 (1993) C24. (c) A.J. Deeming, K.I. Hardcastle and S.E. Kabir, *J. Chem. Soc., Dalton Trans.*, (1988) 827. (d) M.I. Bruce, P.A. Humphrey, O. bin Shawkataly, M.R. Snow, E.R.T. Tiekink and W.R. Cullen, *Organometallics*, 9 (1990) 2910.
- [9] H. Jungbluth, G. Süss-Fink, M. Pellinghelli and A. Tiripicchio, *Organometallics*, 9 (1990) 1670.
- [10] F.S. Livotto, P.R. Raithby and M.D. Vargas, *J. Chem. Soc., Dalton Trans.*, (1993) 1797.
- [11] R. Ros, A. Scrivanti, V.G. Albano and D. Braga, *J. Chem. Soc., Dalton Trans.*, (1986) 2411.
- [12] (a) J.R. Shapley, S.J. Hardwick, D.S. Foose, G.D. Stucky, M.R. Churchill, C. Bueno and J.P. Hutchinson, *J. Am. Chem. Soc.*, 103 (1981) 7383. (b) M.R. Churchill and J.P. Hutchinson, *Inorg. Chem.*, 20 (1981) 4112.
- [13] S.R. Hall, H.D. Flack and J.M. Stewart, *The XTAL 3.2 Reference Manual*, Universities of Western Australia, Geneva and Maryland, 1992.